Efficient Rectifier for Wireless Power Transmission Systems

Efficient Rectifier for Wireless Power Transmission Systems

S. Rotenberg, *Student Member IEEE*, S.K. Podilchak, *Member IEEE*, P.D. Hilario Re, *Student Member IEEE*, C. Mateo-Segura, *Member IEEE*, G. Goussetis, Senior *Member, IEEE*, J. Lee

***Abstract*— This paper describes a full-bridge rectifier and a receiving antenna array for operation within an innovative wireless power transmission (WPT) system. A high-power transmitter using circularly polarized free-space waves and based on retrodirective antenna array technology, is also employed to boost the overall received RF power at the input of the rectenna. To the authors' best knowledge, the proposed rectifier circuit and active antenna configuration is the first demonstration of a high power beam tracking system for WPT scenarios, being different from previously reported near-field coupling and other lower power harvesting schemes. The main focus of our present work is the rectifier design, its bench-top measurements, and operation in such a retrodirective, self-tracking microwave system. A novel approach based on in-phase multitone input signals is also developed to improve rectifier efficiency. The rectifier size is 4.5 cm by 2 cm and can offer more than 86% and 75% RF-to-DC rectification efficiency at 27 dBm for an input signal at 1.7 GHz and 2.4 GHz, respectively. This rectifier circuit component can also be employed in other communication applications or WPT systems. For example, to convert to dc received RF signals or power in the radiating near- and far-field in order to wirelessly charge the batteries of home electronics such as smartphones, tablets or IoT devices.**

***Index Terms* — active antenna rectifier, diode, patch array, rectenna, wireless power transfer**

I. Introduction

Wireless power transfer or transmission (WPT) has been studied over the last few years and it is considered a possible technology to charge any electronic device wirelessly and a variety of applications have been proposed in the literature. For instance, wireless charging by magnetic resonance [1], [2] is widely used in biomedical devices [3] and has been examined for electrical vehicles [4]. Other WPT approaches include magnetic induction by reactive near-field coupling [5]. The alternative technique described in our paper is based on electromagnetic free-space radiation and an efficient rectifier is newly reported for demonstration in such a microwave transmission system (MTS). Applications include the powering of smartphones, wearables, devices for internet of things (IoT) technologies, and other mobile electronics, defining the device under charge (DUC), in such a WPT system.

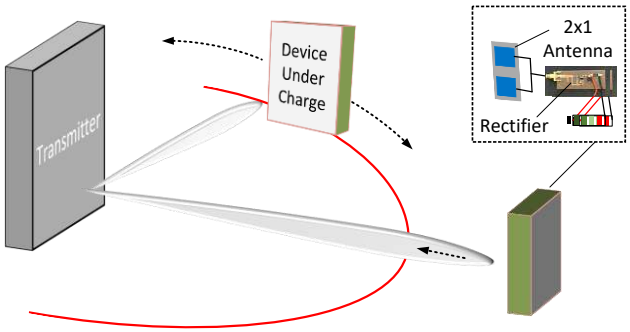

Fig. 1. Developed WPT concept where the device under charge (DUC) can be self-tracked and its batteries charged using the rectenna of this work. Automatic tracking of the DUC is achieved using a 2x1 antenna array (at the mobile unit) as well as by the self-steered radiated fields from the RDA transmitter.

In our experimentally verified MTS, radiated power is directed towards the proposed rectifier circuit which is also connected to a receiver antenna array as illustrated in Fig. 1. This rectenna unit is positioned in the near-field whilst receiving a power level of about 27 dBm at the RF input of the rectifier. This input power level is sufficient to charge a smartphone battery and maintain operation in an idle mode [6]. This can support continuous operation of the mobile, or DUC, when in the vicinity of the MTS.

It should be made clear that the proposed rectifier and WPT system is not intended as a replacement for the conventional wired charging, but can be considered as complimentary as in the adopted DUT scenario. This can improve the quality of the users' experience, and flexibility for device battery charging, instead of relying on previous magnetic induction approaches [1]-[5], which typically require some type of pad or surface technology for more localized WPT, as well as more common wired charging approaches which require ac to dc converters and other power supply circuitry.

Manuscript received Nov. 2018, resubmitted August 2019 and December 2019. Accepted December 27th, 2019. This work was supported by Samsung under the GRO Grant Scheme (Year 1) and the H2020 project CSA-EU.

S. Rotenberg, S. Podilchak, P.D. Hilario, G. Goussetis, and C. Mateo-Segura are with Heriot-Watt University, Institute of Sensors Signals and Systems, Scholl of Engineering and Physical Sciences, EH14 4AS (corresponding author: skp@ieee.org).

Jaesup Lee is with Samsung Advanced Institute of Technology, Samsung Electronics Co., Ltd, Kiheung, Korea. (jaesup2003.lee@samsung.com)

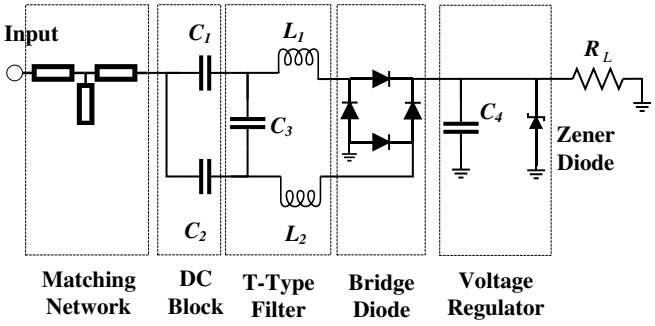

Fig. 2. Circuit schematic overview for the proposed rectifier.

For application testing purposes and for efficient power transfer to our proposed rectenna, (or mobile DUC within the MTS, see Fig.1), and to further minimize free-space path losses, the position of the rectenna is automatically tracked by an active retrodirective beam-steering approach. More specifically, a high-power retrodirective antenna array (RDA) transmitter [7]-[10] which employs active phase conjugating mixers [9], pre-amplifiers, power amplifiers, and separated input/output circularly polarized (CP) patch arrays as in [11]. In our developed MTS for this paper, to enable rectifier testing and WPT system assessment, a network of arrays are employed to generate 2.4 GHz left-handed circularly polarized (LHCP) fields at the RDA for high-power radiation, free-space propagation, and rectification at the DUC.

These CP antenna elements, and the supporting active circuit chains, can improve the received power levels at the RF input of the rectifier and allow for free orientation and movement of the mobile DUC. At the same time our CP-RDA transmitter provides a realistic and application specific MTS measurement environment for the proposed rectifier. Also, in our demonstrated system, the rectenna is co-located with the pilot beacon antenna circuity which generates a 2.5 GHz right-handed circularly polarized (RHCP) signal tone (see Fig. 1) for mobile tracking. In this work we define this rectenna and pilot beacon signal as the receiver module for the MTS, while the RDA, which is a type of heterodyne CP-RDA architecture for high-power re-radiation, is defined as the transmitter module.

Preliminary findings for a much simpler RDA transmitter module were reported in [11] using a 2×1 transceiver antenna array of CP patches printed on a FR4 substrate. Also, a few initial results for the proposed rectifier and MTS where described in [12] considering operation at 2.4 GHz. In this paper we expand on our original findings and fully report the functionality of the rectifier circuit. In addition, we also demonstrate the capability of our rectifier in terms of its possible RF-to-DC conversion efficiency by considering a multi-tone input while also considering lower rectification frequencies below 2.4 GHz.

This dynamic rectifier functionality is important for WPT systems and when aiming to improve the RF-to-DC power conversion efficiency. For example, operating at lower frequencies can allow for further separation between the transmitter and receiver modules because of the reduced free-space path losses. In addition, by considering different frequencies and more complex signals; i.e. beyond simple tones, improved RF-to-DC conversion efficiencies can also be observed. This can enhance the user experience when considering the intended application and within a given range from the RDA transmitter as the DUC can still be powered and its battery level maintained or charged, and possibly at a faster rate, when compared to the single tone input case.

To the authors' knowledge no similar results have been previously reported for a rectifier circuit which can offer such RF-to-DC conversion efficiencies while also demonstrating its MTS capability and rectenna functionality for operation over a multitude of power levels, frequency ranges, and varied input signal types. As further described in the paper, power conversion efficiencies are maintained well above 60% for these scenarios and peak values of 85% are reported. In addition, the proposed rectifier circuit is not limited to the WPT system of this paper but may also be useful for other MTSs as well as more complex WPT system architectures by free-space radiation in the near- and far-field.

II. Design & Optimization Considerations

The main challenges associated with the proposed rectifier design (see Figs. 2 and 3), its measurements, and system investigation are: 1) the efficient conversion of the received RF signal to dc, 2) the need of high power radiation (from the transmitter module) in free-space during rectenna testing, and, 3) the measurement demonstration in an operational MTS.

It should be mentioned that rectifiers have been classically used in power supply circuits (50/60 Hz) offering full-wave rectification and similar versions of our proposed circuit have been commonly used since the 1970's and for WPT [13],[14]. In our work we focus on a low-cost and planar rectifier implementation for microwave frequencies using a bridge diode topology. Similarly, in [15], the efficiency of a bridge diode rectifier operating at 100 MHz and 2.4 GHz for WPT applications was reported. Other structures using diodes have also been developed for WPT. More precisely, one architecture using only two diodes was examined in [16] offering a 3rd harmonic rejection stub which was also explored in [17]. These rectifier structures are able to provide good efficiency (less than 82.5%) and at a lower input power (26.2 dBm [15], 24.7 dBm [16], and 22 dBm [17], respectively) when compared to our work. More specifically, as reported in our paper, we are able to efficiently rectify input RF power levels of more than 27 dBm while also considering different signal types and operational frequencies.

Other rectifiers have also been designed to operate for dual-frequencies albeit at lower power levels. In [18], the reported rectenna efficiently converted the RF received signal at 920 MHz and 2.4 GHz by using a four-stage voltage doubler topology. Moreover, in [19], a printed diode rectenna was

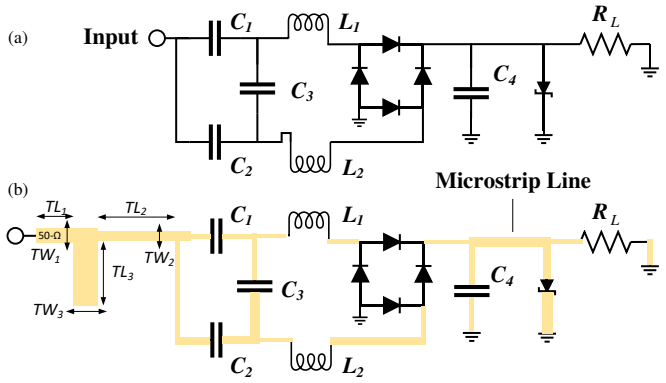

Fig. 3. Circuit models to illustrate the design methodology for the fabricated and measured rectifier (see Fig. 4). The basic circuit was initially optimized with ideal circuit components and without any input matching network (a). Next this input matching network for a 50-Ω impedance was included (defined by TL_1, TW_1, TL_2, TW_2, TL_3, TW_3 using ideal transmission line sections). All possible circuit elements were parameterized and further optimized. This was followed by a realizable structure using transmission lines and an input matching network in microstrip technology (b).

designed in order to convert 19.5 dBm of input power with a good efficiency (84.4%) at 2.45 GHz and 5.8 GHz.

For the rectifier circuit of our work, as well as the WPT system for testing, the designed circuit should be able to efficiently convert different power levels when considering the RF power collected at the receiver module. This is important because the received power level is dependent on the position of the DUC from the transmitter module. Also, the mobile should be able to freely move with limited range restrictions for the best user experience. Hence, the RF power levels received by the rectifier at different distances are not static and thus the rectenna should be able to convert different RF power levels with similar efficiencies to ensure continuous and consistent powering of the mobile DUC.

Previous designs found in the literature lack this overall capability as they typically convert RF power efficiently over a predefined power level and dedicated design frequency. Our rectifier presented in this paper offers an efficiency of over 70% for power levels over 15 dBm between 1.6 GHz and 1.9 GHz, and more than 86% at 27 dBm. At higher frequencies, our proposed rectifier offers similar efficiency values for the RF-to-DC power conversion. For example, at 2.4 GHz an efficiency of 76% can be observed at 26 dBm and over 60% for RF input powers ranging from 15 dBm to 29 dBm.

Following the works presented in [20]-[22], which studied the use of chaotic and multi-sinusoidal signals to enhance rectification operation, we further improve RF-to-DC efficiency in our proposed rectifier. As it will be shown, a comparison between the single and the multitone input approach is presented at 2.1 GHz and 2.4 GHz. This study is important to accommodate for more complex WPT configurations and other possible MTSs which consider different propagating signals.

A. *Rectifier Circuit Overview and Design Approach*

The rectifier circuit schematic is illustrated in Figs. 2 and 3, and the fabricated prototype is shown in Fig. 4. The structure comprises five different blocks. Firstly, at the input port where the RF signal is collected, the matching network can be found. Its main purpose is to minimize reflections and offer 50-Ω impedance matching for the required input power levels and frequency ranges, as described above, whilst considering all circuit components and the active impedance matching of the diodes. This matching network is defined by an open ended single-stub tuner offering advantages in terms of simplicity and the fact that lumped elements are not needed. This can reduce fabrication costs.

After the matching section, there is a dc block composed of two capacitors (C_1 and C_2) to minimize any dc signal passing through to the bridge diode. Next, a T-type low-pass filter is applied (C_3, L_1 and L_2) to recover the efficiency degradation caused by the junction capacitance of the bridge diodes. The last block is composed of a smoothing capacitor (C_4) as well as a Zener diode which acts as a regulator to reduce the ripples observed at the load resistance (R_L).

The design approach for the rectifier is briefly illustrated in Fig. 3. The first step was to identify from available electronics suppliers the most appropriate diode architecture in order to convert a high RF input power (in excess of 27 dBm) to dc and ensuring high rectification efficiency at the required frequencies. A bridge diode configuration was selected. The second step was to define the basic schematic of the circuit within an RF circuit simulator (AWR Microwave Office). Then the capacitances, inductances, bridge diodes, Zener diode, and load resistor where included to initially validate the circuit architecture without any matching network (see Fig. 3(a)). Then these circuit elements were all parameterized and their values optimized to increase the RF-to-DC rectification efficiency and reduce the ripples at the output whilst considering a single 27 dBm RF input tone signal at 2.4 GHz.

The next step in the rectifier design was to include in the simulator an input transmission line section as well as the open ended single-stub matching network. These components were

TABLE I
RECTIFIER COMPONENT VALUES AND MATCHING SECTION LINE LENGTHS

	Component	Value
Rectifier Circuit Elements	C_1	1.9 pF
	C_2	0.4 pF
	C_3	470 nF
	C_4	470 nF
	L_1	8 nH
	L_2	3.9 nH
	R_L	669 Ω
Matching Network	TL_1	10.0 mm
	TW_1	4.9 mm
	TL_2	2.9 mm
	TW_2	3.1 mm
	TL_3	4.6 mm
	TW_3	2.3 mm

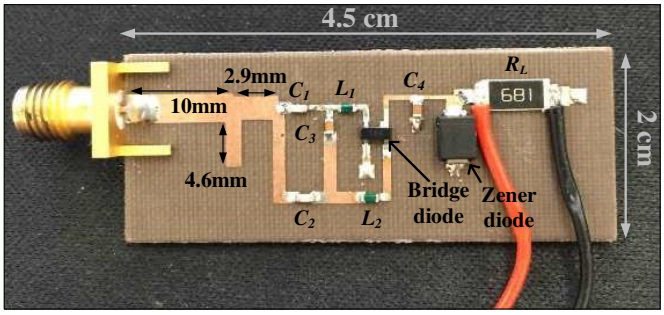

Fig. 4. Photograph of the fabricated and measured rectifier.

initially defined by three ideal transmission lines. At this step, moreover, these three transmission line sections all had the same width (which defined a 50-Ω characteristic impedance), but with different lengths. Then all circuit values and transmission line lengths were optimized again. More specifically, the lengths TL_1, TL_2 and TL_3 were considered as variables to tune along with the different lumped elements within the rectifier. Also, via hole placements for ground terminations where included in the simulations. Basically, all possible circuit dimensions and values were further refined to minimize reflection losses, increase RF-to-DC rectification efficiency, and reduce ripple for a 2.4 GHz single tone at the input and with a power of 27 dBm.

Then the remaining connections between the other circuit components were all replaced with microstrip (see Fig. 3(b)). It should be mentioned that simulations were completed using the full-wave EM solver within AWR. All possible values and the microstrip line dimensions in the circuit, except for the matching network (which were still ideal transmission lines at this step), were parametrized and considered as variables in the rectifier optimization process. This resulted in about 60 variables within the simulator to reduce reflections, increase efficiency, and reduce the output ripple whilst considering the largest possible range of power input at 2.4 GHz.

A last optimization step was finally made which now included all possible dimensions for the matching network whilst considering microstrip. It should be mentioned that the input transmission line width (TW_1) was fixed for a 50-Ω characteristic impedance while its length was maintained beyond about 1 cm for SMA connectivity. During this step the motivation was to increase the possible input matching bandwidth for a large range of input power levels and optimize the efficiency while also reducing the output ripple.

Throughout this design process, it was realized that by varying all the parameters of the matching network, along with the other variables within the circuit simultaneously, the general frequency of operation for the rectifier could be tuned. We also observed that the circuit harmonics could be exploited realizing a more dynamic response for the rectifier. More specifically, the best results in terms of efficiency, minimized output ripple and reflection coefficient over frequency, and when considering different input power levels, was when the first harmonic (originally design to be centered at 2.4 GHz as described above) and its second harmonic, were reduced in frequency. Basically, when the first and second harmonics were positioned at about 1.7 GHz and 2.4 GHz, respectively. This response for the rectifier was also found to be useful for the above mentioned multitone input study, in that improved efficiency was possible when compared to a single input tone for some relevant cases.

The rectifier was manufactured using a base substrate of Taconic material (TLY-5) with a relative dielectric constant of 2.2 and a thickness of h = 1.6 mm. The components used are SMD Ceramic Multilayer MLCC capacitors, inductors and a chip SMD resistor. Their values are referenced in Table I. The bridge is composed of Schottky diodes (Avago HSMS-2828) with a series resistance R_S = 7.8 Ω, a breakdown voltage V_b = 26.7 V and a junction capacitance C_{j0} = 0.649 pF (at 0 V). The Zener diode is the 1SMB5935BT3 model from ON Semiconductor. It should be mentioned that our main reason to select the Avago Schottky diode for the bridge was mainly related to its high breakdown voltage V_b of 26.7 V. There is also a limitation on the input power of the rectifier, which is due to the breakdown voltage of the diode in that the voltage junction V_j cannot be higher than V_b. Basically, during the design we needed to ensure that the input junction voltage was well below 26.7 V whilst considering the input power level of 27 dBm.

A. *Receiver Design*

A 2.4 GHz LHCP 2x1 patch antenna array with a gain of 10 dBic, offering 50-Ω impedance matching and a Wilkinson power combiner have been designed and fabricated (see Fig. 5) using the same substrate as the rectifier. The rectifier collects the RF power at the output of the Wilkinson power combiner for conversion to dc when considering measurements within the MTS (see Fig. 1). Also, we define the combination of the receiver antenna array, the power combiner, and the rectifier, as the rectenna. It should be mentioned that for both the receiver array and the combiner, input reflection coefficient values were well below -20 dB (all results not shown for brevity).

III. Rectifier Simulation Results and Measurements

The rectifier was designed and simulated using AWR Microwave Office. The dc output power was computed using

$$P_{out} = \frac{V^2}{R_L} \qquad (1)$$

where V is the potential difference across the resistive load R_L. The rectifier efficiency is defined and computed as the ratio of the dc output power to the input power of the RF signal

$$Eff = \frac{P_{out}}{P_{in}} \text{ x } 100\% \qquad (2)$$

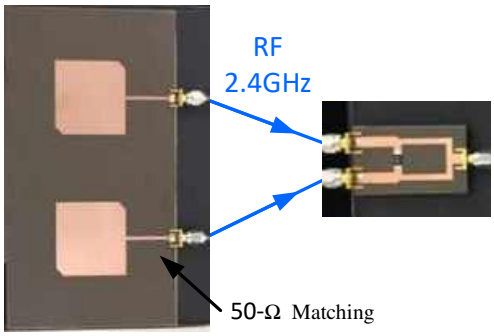

Fig. 5. The 2x1 patch array with a Wilkinson power combiner for operation at 2.4 GHz defining the receiver array and the RF power combiner for the receiver module.

In Figs. 6, 7 and 8 the simulated input and output voltages for the rectifier are compared. Three cases were initially studied (see Fig. 6): the rectifier without the voltage regulator block, the rectifier with the voltage regulator block (considering only the smoothing capacitor C_4), and the rectifier with the voltage regulator block as seen in Fig. 2. The RF input voltage is shown for the dotted purple line. It can be observed that with these added components, the output voltage ripple reduces. It can also be observed from these simulations, that the effect of the voltage regulator block is two-fold. On one hand, when a smoothing capacitor is used (see the blue line in Fig. 6), the variation of the rectified current output is reduced which in turn improves the average dc output of the rectifier.

On the other hand, when the Zener diode is employed as a voltage stabilizing device (see red line in Fig. 6) the output signal ripple is further reduced. Considering an input RF power of 27 dBm at 2.4 GHz, the simulation shows that the dc voltage fluctuates between 16.2 V and 17.1 V in Fig. 7 while the current varies between 23.9 mA and 25.2 mA. A similar response was also simulated considering a 1.7 GHz input tone. These minor variations of voltage and current can offer stable dc voltage rectification and we consider these output ripples suitable for the MTS studied in this paper.

The T-type filter rejects the higher harmonics that can be generated at the output of the rectifier. Fig. 8 shows the voltage level of the harmonics in the output at 1.6 GHz, 1.7 GHz, and 1.8 GHz in (a), and 2.3 GHz, 2.4 GHz, and 2.5 GHz in (b). In all cases, voltage levels are below 1 V, and as expected, most of the power is observed at dc. It is interesting to note that when the filter is removed (red line) part of the power goes to the first, second, third, and fourth harmonics and maximum values of about 3 V can be observed. When the filter is included in the simulation (blue line), the power is not lost in the higher harmonics and consequently, a higher voltage appears at the fundamental harmonic dc. For example, improvements of 2 V or more can be observed with the filter.

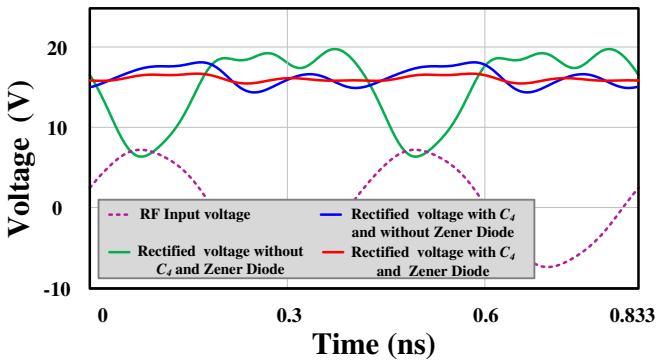

Fig. 6. Simulated input and output voltage of the rectifier for an RF input power of 27 dBm at 2.4 GHz. It can be observed that output voltage ripples are reduced when compared to the input RF with C_4 and the Zener diode.

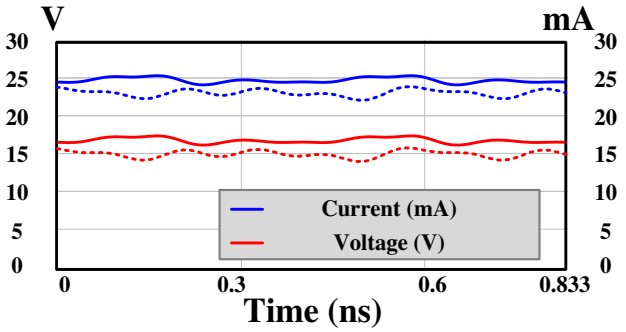

Fig. 7. Simulated output voltage and current for the rectifier for an RF input power of 27 dBm at 1.7 GHz (dashed line) and 2.4 GHz (continuous line).

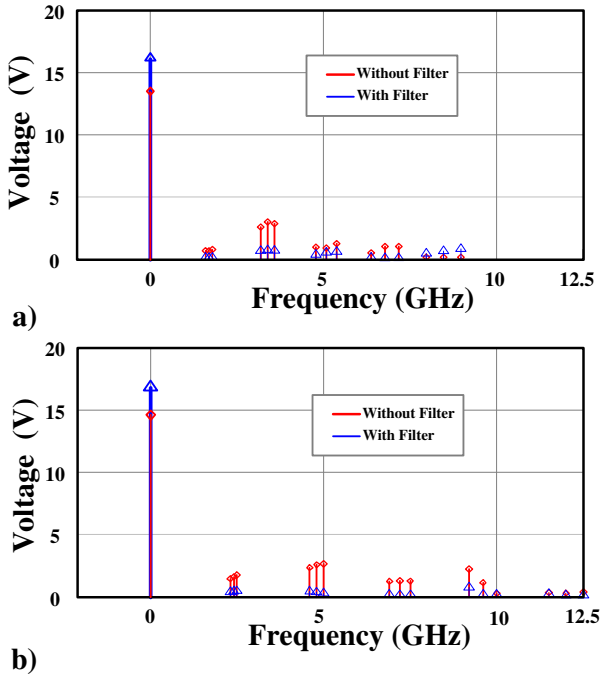

Fig. 8. Comparison of the harmonics at the output of the rectifier with and without the filter considering an input RF power of 27 dBm at a) 1.7 GHz and b) 2.4 GHz.

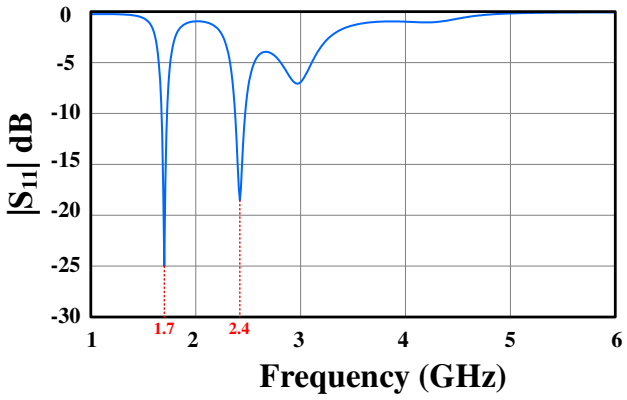

Fig. 9. Simulated reflection coefficient $|S_{11}|$ of the rectifier considering an input power of 27 dBm.

In Fig. 9 the simulated reflection coefficient for the rectifier over a large frequency range is reported. As can be observed, good matching is achieved at 1.7 GHz and 2.4 GHz where values of $|S_{11}|$ are equal to -25 dB and -18 dB, respectively. It should be mentioned that results reported in Figs. 6 to 9 were obtained considering a fixed value for the load impedance, R_L (see Table I). However, a battery can have a variable impedance depending on its charging state and size, also for example, when considering various DUCs; i.e. smartphone or small IoT device batteries. To further investigate the rectifier operation given these possible cases for the adopted DUC charging scenario (see Fig. 1), RF-to-DC conversion efficiency simulations are shown in Fig. 10 for different load impedance values. A wide range of power levels and frequencies are considered. It can be observed that for R_L between 100 Ω and 1k Ω, RF-to-DC rectification efficiency values are well above 50%, and more than 80%, for the optimized frequencies and power levels.

In terms of battery size, it is well known that the load resistance will change depending on the DUC. In [23] (see Fig. 4), an investigation of various battery resistances for possible DUCs was reported. In particular, an impedance range between 100 and 1k Ω is likely for coin-size batteries supporting IoT devices [23]. This suggests that 669 Ω is a typical, mid-range load resistance that can be representative of the battery to be charged for the DUC.

Measurements were carried out at the microwave lab at Heriot-Watt University using a calibrated power generator and a signal source (Keysight 4-Port N5225B PNA) to generate the desired input signal. This input signal was then amplified with an RF power amplifier and studied using a vector signal analyser (Keysight N9030B PXA) as shown in Fig. 11. The output dc signal was measured at the load resistance.

The rectification efficiency for different input power levels (10 dBm to 28 dBm) at 1.7 GHz and 2.4 GHz was also analysed. Fig. 12 shows good agreement between the simulated and measured results. It can be observed from this plot that the designed rectifier converts efficiently (above 60%) for a range of power levels between 10 dBm to 28 dBm

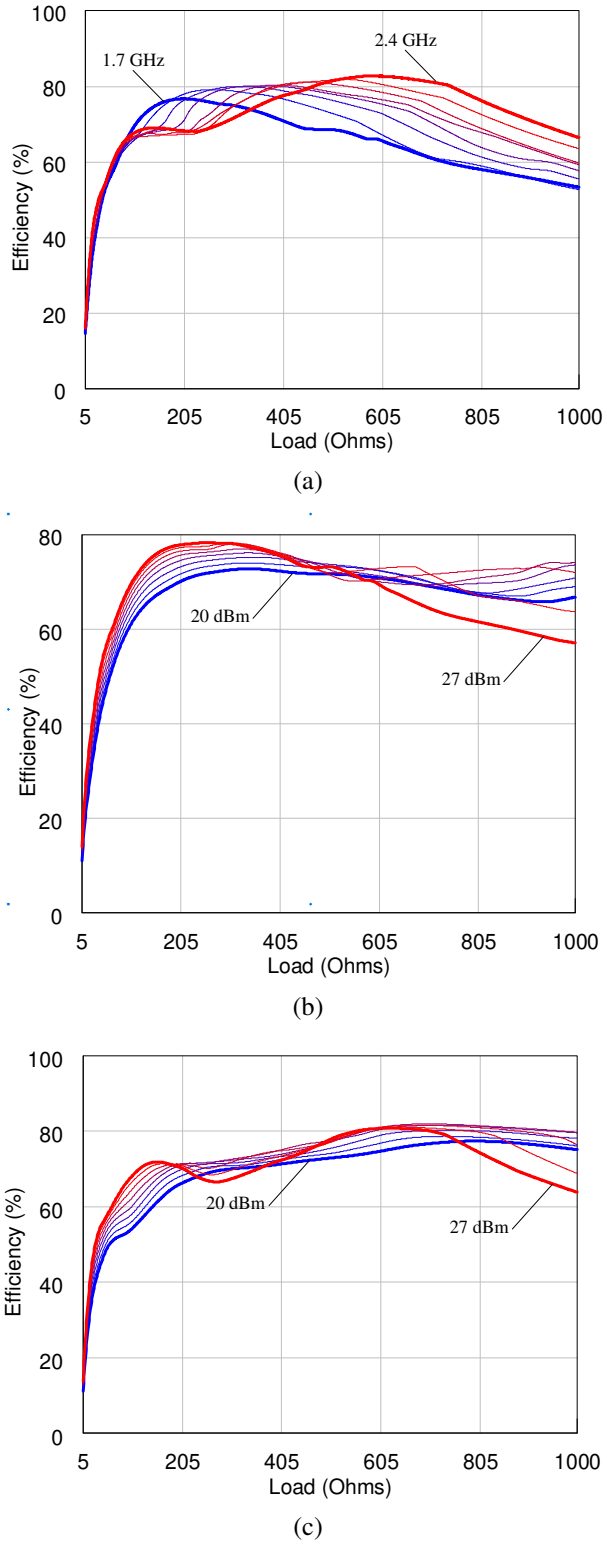

Fig. 10. Rectifier efficiency compared for different load values, R_L: from 1.7 to 2.4 GHz considering 27 dBm (a), different input RF power levels at 1.7 GHz and 2.4 GHz, (b) and (c), respectively.

and 15 dBm to 28 dBm at 1.7 GHz and 2.4 GHz, respectively.

Given this diversity in the rectification efficiency, the DUC (when considering the intended WPT application scenario),

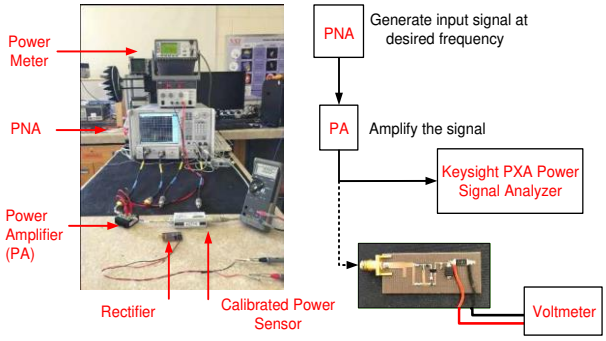

Fig. 11. Bench top rectifier measurement setup.

will be able to move freely in 3D space offering efficient charging of the mobile battery at different ranges from the transmitter. Thus, depending on the distance of the mobile from the RDA transmitter, the rectifier receiver module must be able to convert different RF power levels to dc. For example, more power will be rectified at the rectenna when the receiver module is closer to the RDA transmitter by Friis' frees-pace path loss formula. Therefore, it was crucial in the design of the rectifier to efficiently convert power (from RF to dc) over a large range of input power levels. Also, the minimum power level, 10 dBm at 1.7 GHz, offers more than 50% rectification efficiency. Lower power levels have not been further considered in this work, as we deem this power level insufficient to transfer power to a DUC battery.

It can also be observed that the rectifier efficiency is frequency dependant and increases with input power levels reaching a maximum (which is dependent on the breakdown voltage of the diodes). However, within the range of frequencies examined in Fig. 13, from about 1.65 GHz to 1.9 GHz, the efficiency remains relatively stable (above 70% and 80%) respectively considering an 18 dBm and 27 dBm input RF power level.

In view of the intended WPT application (see Fig. 1), this varied power level and broadband performance offers an efficient conversion to dc, even when the electronic mobile device (or receiver module) is on the move around the transmitter module. For example, if the rectenna (or mobile DUC receiver unit) is moving with some non-zero velocity, it will receive the radiated high-power signal at a slightly different frequency and power level than the one transmitted by the RDA due to the Doppler Effect. Given this range of frequencies (1.7 GHz and 2.4 GHz) with maintained rectification operation, the receiver module can freely move and rotate due the radiated CP fields of the transmitter module. This important rectifier functionality can enhance the user experience as the mobile battery can still be charged within a given distance from the transmitter.

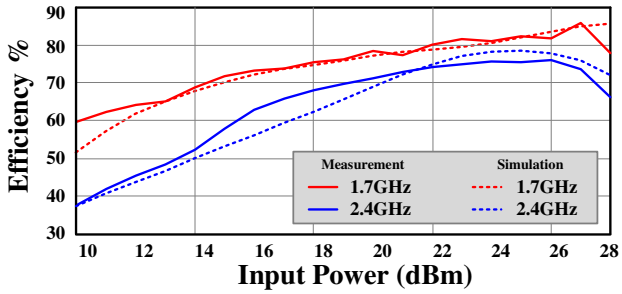

Fig. 12. Measured and simulated RF-to-DC conversion efficiency versus the input power at 1.7 GHz and 2.4 GHz.

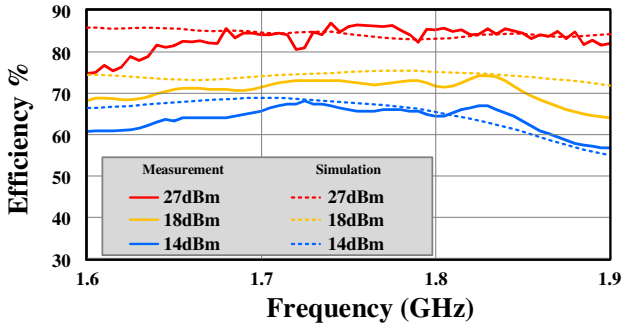

Fig. 13. Measured and simulated RF-to-DC conversion efficiency versus frequency at three different power levels.

Table II compares the characteristics, and conversion efficiencies of our work and other rectifiers reported in the literature. It can be observed that our proposed rectifier circuit offers an improvement when compared to other rectifiers found in the literature, in terms of rectification efficiency and for the highest input RF power level.

IV. RF-DC EFFICIENCY OPTIMIZATION USING MULTI-TONE SIGNALS

It has been previously studied that the efficiency of a rectifier can be further improved when two-tone and multi-toned signals are employed [22], [24] or when using power optimized waveforms [25]. It was further examined in [26] that when signals with a high peak to average power ratio are considered, an improvement of the RF-to-DC conversion efficiency can be observed when compared to a continuous wave (CW) signal with the same average power.

Following these developments, we further investigate the performance of our rectifier circuit considering a multi-tone input signal with a bandwidth of 35 MHz, as illustrated in Fig. 14. In particular, we study 8-tones (all in phase) separated by 5 MHz at the RF input, centred at 2.4 GHz, having a total average power equivalent to the power of the CW tone signal examined previously; i.e. 27 dBm at 2.4 GHz. It should be mentioned for this multi-tone study that the RMS value for the signals are equal to $N / \sqrt{2} \sim 1.4$, with a Crest Factor of $\sqrt{2N} = 4$, while the peak-to-average power ratio (PAPR) is $10\log 2N \sim 1.2$ dB. Here N (= 8) which defines the total number of tones.

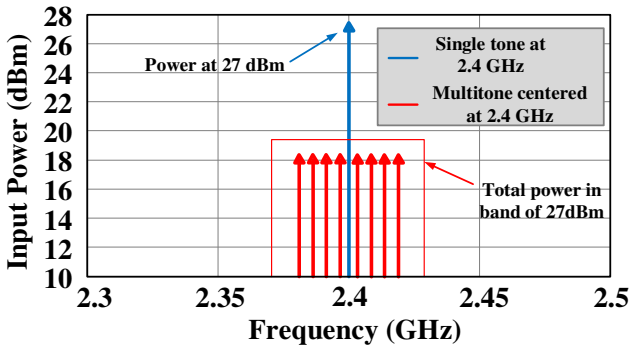

Fig. 14. Illustration of the multi-tone input for rectifier testing.

The operation of the rectifier considering a multi-tone input, can be further understood by studying the efficiency of the rectifier versus frequency for a single-tone (0º relative phase difference [22]) at the RF input for different power levels (see Figs. 15 and 16). Taking 2.1 GHz as an example, it can be observed that that the efficiency reaches a local minimum for 26 dBm and 27 dBm. If a multi-tone input signal, as the one shown in Fig. 14 is employed (but centred at 2.1 GHz), the rectifier will allow for the average RF power to be converted within the defined 35 MHz bandwidth rather than at an individual frequency. For this particular case, the resulting efficiency will be higher for a multi-tone input, as shown in Fig. 15(a), when compared to a single-tone. For example, it can be observed that the efficiency increases by about 13% and for increased input RF power levels; i.e. 27 dBm.

The case of 2.4 GHz is also studied. In Fig. 16, a local maximum can be observed at 26 dBm and 27 dBm and a minimum at the other input power levels. By studying the measurements in Fig. 15(b), it can be observed that for input power levels below than 14 dBm (i.e. where the local minima are found) the measured efficiency is higher for the multi-tone input case. Conversely, for input power levels larger than about 14 dBm, a single tone excitation is the preferable RF input signal. This is because the RF-to-DC conversion efficiency is more than 60% for input power levels of 16 dBm to 28 dBm.

The improvement in rectification efficiency due to the multi-tone input can be further explained by observing the simulated reflection coefficient for different input RF power levels as shown in Fig. 17. Due to the active rectifier device, the reflection coefficient can change and is dependant on the input RF power levels. For example, reflection coefficient values are below about -15 dB at 1.7 GHz and 2.4 GHz for RF input power levels greater than 12 dBm while higher reflections are observed at 2.1 GHz for a 27 dBm input tone; i.e. values are about -2 dB and -10 dB for input RF power levels of 18 dBm and 27 dBm, respectively. Moreover, by considering the same example in Fig. 15(a), it can be observed that in order to achieve improved rectification efficiency with a multi-tone input signal, it is suggested to inject 8 tones, each with a power of 18 dBm centred at 2.1 GHz (defining a total power of 27 dBm) rather than a single tone at 2.1 GHz with a power of 27 dBm. This is due the improved matching that can be observed for an 18 dBm input

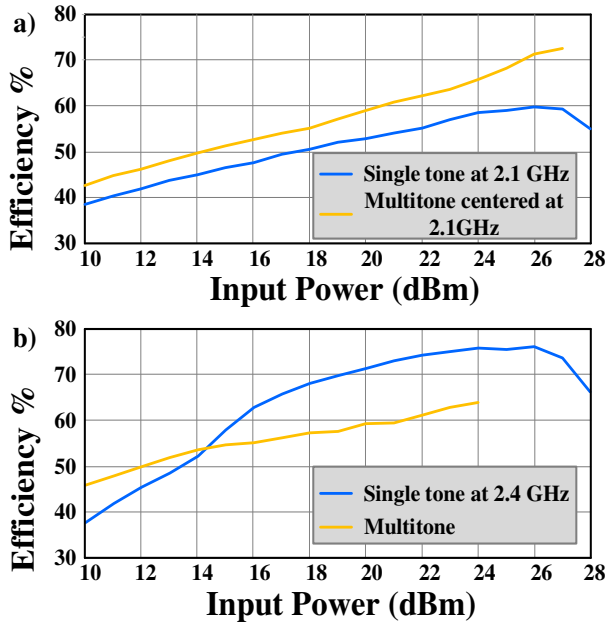

Fig. 15. Measured RF-to-DC conversion efficiency versus input RF power. A comparison between a single tone input and a multi-tone input is reported at (a) 2.1 GHz and (b) 2.4 GHz.

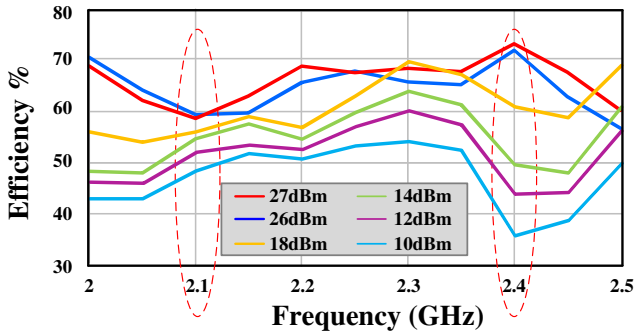

Fig. 16. Measured RF-to-DC conversion efficiency versus frequency at different power levels considering a single-tone input.

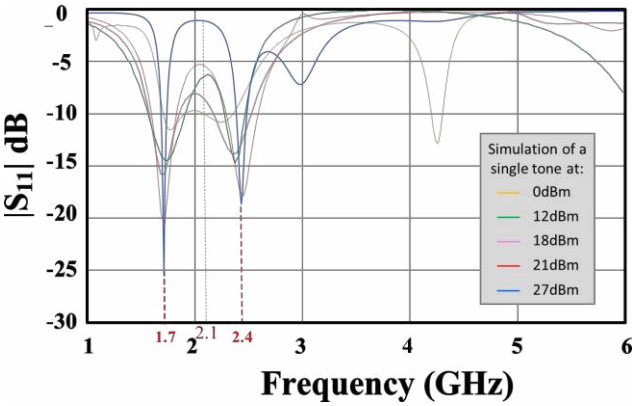

Fig. 17. Reflection coefficient at different power levels considering a single-tone input.

signal.

In an effort to optimize the RF-to-DC conversion efficiency, this varied RF input signal approach can be envisioned as part of a smart MTS and electronically programmed for WPT which is capable to switch between single and multi-tone input signals according to the observed local minima or maxima rectifier efficiency. This in turn will provide a WPT system capable of providing high RF-to-DC conversion efficiency for a wide range of input power levels which is related to different positions of the mobile DUC.

V. System Measurements

To enable rectifier testing and to study its performance within the WPT system, the rectifier was measured in an anechoic chamber as shown in Fig. 18. Four receiver elements were employed for the CP-RDA, while at transmit, a network of 4 arrays (not 2 as in Fig. 5 from [11]) were adopted.

This transmitter module used for system rectifier testing generates a 2.4 GHz left-handed circularly polarized (LHCP) field using a 4x4 array configuration which was sub-divided into four sections (see Fig. 18). It was designed using microstrip technology, and each of the patch antennas are fed in series within the corresponding sub-array. The total realized LHCP gain is around 18 dBic with an axial ratio (AR) of less than 2 dB at broadside. The dc power consumption of the RDA was about 15 W. This was calculated considering the four driver amplifiers (ZFL-2500+, rated supply 5V, 0.22A) and the four power amplifiers (TQP9111, rated 5V, 0.545A) connected to the four sub-arrays. Additionally, the effective isotropic radiated power (EIRP) for the RDA transmitter was 55 dBm and the RF power delivered into the antenna sub-arrays was around 37 dBm (5W).

Such a system was made for high-power radiation and rectifier testing at the receiver module**.** Also, since the RDA has been designed at 2.4 GHz the rectifier system testing and the performance of the circuit has been measured only at 2.4 GHz within the MTS. During the measurements, the rectifier was first connected to a 2-by-1 receiver patch antenna array forming the rectenna during the experimentation for proof of concept. System measurements were then carried out in the near-field and the far-field zone. In Fig. 19, the received RF power (input power of the rectifier) and the resultant dc power (output power of the rectifier), is shown at broadside from 40 cm to 75 cm and this range is actually in the reactive near-field (other far-field range tests were also completed, but not reported due to brevity). As can be observed, the RDA was able to direct RF power to the rectenna unit enabling the rectifier to convert the RF power to dc power. In particular, the rectifier provides around 250 mW (24 dBm) of dc power at 75 cm with more than 350mW (> 27 dBm) between 40 cm and 60 cm.

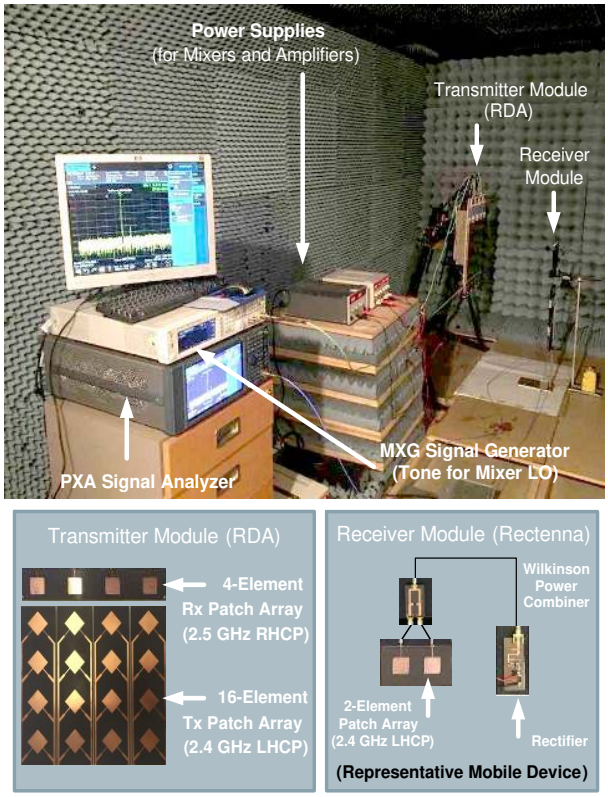

Fig. 18. System measurement for the rectenna. The supporting RF chains for the transmitter include mixers (LTC5549 from Linear Technology), driver amplifiers (ZJL-4G+), power amplifiers (TQP9109 from Triquint) as well as in-house printed hybrid couplers for the generation of CP fields.

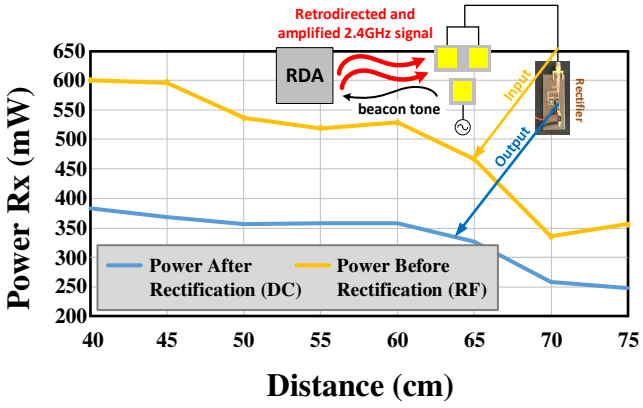

Fig. 19. Measured received power at RF and dc at broadside for a range of distances from the RDA transmitter module.

In Fig. 20 measurements are reported showing the tracking capability of the rectenna and its operation within the MTS; i.e. when the receiver module is rotated around the transmitter module at a fixed range of 50 cm. It can be observed that the 3 dB beamwidth is approximately 70˚. The dc power rectified versus the incoming angle was also recorded and is represented by the green line in the figure.

The reduction in power for this curve with respect the RF

TABLE II
COMPARISON TABLE BETWEEN DIFFERENT RECTIFIER CONFIGURATIONS

Reference	Frequency (GHz)	Substrate	Size (cm)	P_{in}(dBm) at maximum efficiency	Topology	Maximum Efficiency (%)
[27]	5.2/5.5	Duroid ε_r=2.2	6.2 x 3	10	Single diode	57.3
[28]	5.8	Duroid ε_r=2.94	6.5 x 1	18	Single diode	68.5
[29]	5.8	Duroid ε_r=2.2	-	16.1	Diodes in parallel	73.3
[30]	2.4	Duroid ε_r=2.33	-	10	Single diode	77.8
[18]	0.92/2.4	FR4 ε_r=4.4	3 x 1.5	15	Four-stage voltage doubler topology	78
[16]	2.45	FR4 ε_r=4.4	3 x 3	24.7	Diode Pair	78
[15]	2.4	PTFE Board ε_r=2.6	4.5 x 4.8	26.2	Bridge Diode	80
[31]	5.8	Duroid ε_r=2.2	-	16.9	Single diode	82
[17]	2.4	FR4 ε_r=4.4	4.5 x 4.5	22	Pair of Diode	82.3
[19]	2.4/5	Duroid ε_r=2.33	6.2 x 1	19.5	Single diode	84.4
This Work	**1.7/2.4**	**Taconic TLY-5 ε_r=2.2**	**4.5 x 2**	**27**	**Bridge Diode**	**86**

ones, is related to the efficiency of the rectifier. In addition, the received RF power is greater than 300 mW for about a 70˚ angular range (from about -35˚ to +35˚). To the authors' knowledge there has not been any similar rectifier reported in the literature demonstrating its operation in a MTS for WPT applications, in particular, which can support the continuous powering of various DUC such as smartphones, IoT devices and other portable electronics.

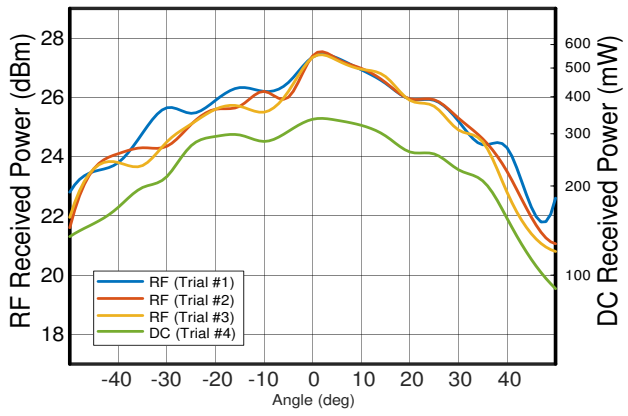

Fig. 20. Measured tracking capability of the MTS and rectenna at 2.4 GHz versus angle for a fixed range of 50 cm from the transmitter module. Three measurement trials were completed whilst using a Keysight PXA Spectrum Analyzer at the receiver module (Trials #1 to #3, left axis) and also at the output of the rectifier; i.e. the power measured across the load R_L (Trial #4, right axis).

VI. HEALTH CONSIDERATIONS

Given that high RF power is being radiated in the presence of human bodies, it is important to address any possible human health risks and the related power transmission regulations. It should be mentioned firstly that the low energy levels associated with microwave radiation at 2.4 GHz, the power levels are usually not considered dangerous and should not cause ionization of atoms and molecules thus causing damage to human deoxyribonucleic acid (DNA) and other tissue [32]-[36].

It is however recognized that certain RF power densities can have some possible effects to humans. To address these concerns, several studies have been initiated to determine the safe levels of exposure to RF radiation for the general public. Several guidelines and standards have been issued by the IEEE, the American National Standards Institute (ANSI), the International Commission on Non-Ionizing Radiation Protection (ICNIRP), The Federal Communications Commission (FCC), and the National Council on Radiation protection and Measurements (NCRP) [30]. These standards are expressed as a power density in mW/cm^2. The ANSI/IEEE/FCC exposure standard is limited at 1.2 mW/cm^2 at the considered frequency and the ICNIRP/NCRP are limited at 0.57 mW/cm^2 for 900 MHz operation. These organizations admit that at a higher power density (4 mW/cm^2) there is no evidence or confirmation of any effects to human tissue or DNA. Moreover, to further quantify these power levels, the specific absorption rate (SAR) is commonly used to further define safety standards and is expressed in W/kg. For

example, it has been established by the Council of the European Union for RF energy absorption [33]-[36] that the SAR should not extend 2.0 W/kg for the human body.

In this research paper, the potential harm of the proposed WPT technology has been carefully considered for the maximum value of the received RF power (27 dBm or 0.5 W). In particular, this value has been selected in order to respect the aforementioned standards. For example, by considering the effective surface dimension of the patch antenna at the receiver module (which has a dimension of 20 cm by 15 cm) it has been calculated that the power density will not exceed 1.66 mW/cm^2 which is well below 4 mW/cm^2. Moreover, the range for the MTS has been considered to be equal or greater than 50 cm to fulfil these constraints, and in particular, during the RDA and rectifier design mainly to ensure safe RF exposure to the human body.

Additional safety circuitry is recommended for the proposed MTS (RDA and rectifier) to ensure individuals are not exposed to unsafe RF power levels. For example, proximity sensors could be put in place to turn off the RDA transmitter or reduce the transmit power when users are less than 40 cm away or similar. Also, given the noted design range of 50 cm and power levels for the WPT system, the SAR has been estimated to be around 1.76 W/kg, by considering an average density of a human body of 945 kg/m^3. This value of 1.76 W/kg is well below the recommended safety standard of 2.0 W/kg.

VII. Conclusions

An optimized full-bridge rectifier using diodes has been presented in this paper. It has been tested on a lab bench and in a WPT system using free-space waves from a transmitter module in order to rectify RF power and to demonstrate the potential application of wireless charging for batteries within various mobile devices under charge.

The designed input RF power level of about 27 dBm can support continuous operation of the DUC when in the vicinity of the MTS. However, the proposed rectifier and WPT system is not intended as a replacement for more conventional wired charging approaches, but complimentary, in that the DUC battery could continuously charge when in the vicinity of the developed MTS. This can support uninterrupted operation and less battery replacement and charging interventions for smartphones or IoT devices for example, enhancing DUC functionality and user experience.

The optimized and experimentally tested rectifier features a peak conversion efficiency of 86% and it is tested within the microwave system which is defined by an innovative transmitter based on an active circularly polarized 2.4 GHz retrodirective antenna array. Converted dc values in the near-field are above 24.7 dBm. In addition, simulations and measurements show good agreement for the rectifier in terms of RF-to-DC conversion efficiencies and minimal dc voltage and current ripple, whilst considering a range of power levels, battery load types, and input frequencies. This makes the active rectifier circuit suitable for many applications that require WPT, such as smartphones, IoT devices, wearables and other home electronics. Future work can include the design of a new dual-band RDA and other dynamic transmitter systems for WPT applications whilst also considering data communications. This can enhance mobile DUC charging capability and operational features of the MTS.

References

[1] A. Munir and B. T. Ranum, “Wireless power charging system for mobile device basd on magnetic resonance coupling,” in 2015 International Conferenceon Electrical Engineering and Informatics (ICEEI), Aug 2015, pp. 221–224.

[2] J. Garnica, R. A. Chinga and J. Lin, "Wireless Power Transmission: From Far Field to Near Field," in Proceedings of the IEEE, vol. 101, no. 6, pp. 1321-1331, June 2013.

[3] P. Li and R. Bashirullah, "A Wireless Power Interface for Rechargeable Battery Operated Medical Implants," in IEEE Transactions on Circuits and Systems II: Express Briefs, vol. 54, no. 10, pp. 912-916, Oct. 2007.

[4] Chwei-Sen Wang, O. H. Stielau and G. A. Covic, "Design considerations for a contactless electric vehicle battery charger," in IEEE Transactions on Industrial Electronics, vol. 52, no. 5, pp. 1308-1314, Oct. 2005.

[5] H. Hirayama, Y. Okuyama, N. Kikuma and K. Sakakibara, "Equivalent circuit of induction fed magnetic resonant WPT system," 2011 IEEE MTT-S International Microwave Workshop Series on Innovative Wireless Power Transmission: Technologies, Systems, and Applications, Uji, Kyoto, 2011, pp. 239-242.

[6] A. Carroll and G. Heiser. 2010. "An analysis of power consumption in a smartphone," in Proceedings of the 2010 USENIX conference on USENIX annual technical conference (USENIXATC'10). USENIX Association, Berkeley, CA, USA, 21-21.

[7] R.Y. Miyamoto and T. Itoh, “Retrodirective arrays for wireless communications,” IEEE Microwave Magazine, vol. 3, no. 1, pp. 71–79, 2002.

[8] L. V. Atta, “Electromagnetic Reflector,” Patent, 1959.

[9] C. Pon, “Retrodirective array using the heterodyne technique,” IEEE Transactions on Antennas and Propagation, vol. 12, no. 2, pp. 176–180, 1964.

[10] N. Buchanan and V. Fusco, “Developments in retrodirective array technology,” IET Microwaves, Antennas & Propagation, vol. 7, no. 2, pp. 131–140, 2013.

[11] P. D. H. Re, S. K. Podilchak, S. Rotenberg, G. Goussetis and J. Lee, "Retrodirective antenna array for circularly polarized wireless power transmission," *2017 11th European Conference on Antennas and Propagation (EUCAP)*, Paris, 2017, pp. 891-895.

[12] S. Rotenberg, P. D. H. Re, S. K. Podilchak, G. Goussetis and J. Lee, " An Efficient Rectifier for an RDA Wireless Power Transmission System Operating at 2.4 GHz," 2017 32th International Union of Radio Science (URSI), Montreal, 2017, pp. 1-3.

[13] K. Huang and X. Zhou, "Cutting the last wires for mobile communications by microwave power transfer," in IEEE Communications Magazine, vol. 53, no. 6, pp. 86-93, June 2015.

[14] W. C. Brown, "The History of Power Transmission by Radio Waves," in IEEE Trans. Microw. Theory Techn., vol. 32, no. 9, pp. 1230-1242, Sep 1984.

[15] M. Ito et al., "High efficient bridge rectifiers in 100MHz and 2.4GHz bands," 2014 IEEE Wireless Power Transfer Conference, Jeju, 2014, pp. 64-67.

[16] T. C. Yo, C. M. Lee, C. M. Hsu and C. H. Luo, "Compact Circularly Polarized Rectenna With Unbalanced Circular Slots," in IEEE Transactions on Antennas and Propagation, vol. 56, no. 3, pp. 882-886, March 2008.

[17] J. H. Chou, D. B. Lin, K. L. Weng and H. J. Li, "All Polarization Receiving Rectenna With Harmonic Rejection Property for Wireless Power Transmission," in IEEE Transactions on Antennas and Propagation, vol. 62, no. 10, pp. 5242-5249, Oct. 2014.

[18] Qiang Zhao et al., "Dual-band antenna and high efficiency rectifier for RF energy harvesting system," 2015 IEEE 6th International Symposium on Microwave, Antenna, Propagation, and EMC Technologies (MAPE), Shanghai, 2015, pp. 682-685.

[19] Young-Ho Suh and Kai Chang, "A high-efficiency dual-frequency rectenna for 2.45- and 5.8-GHz wireless power transmission," in IEEE Trans. Microw. Theory Techn., vol. 50, no. 7, pp. 1784-1789, Jul 2002.
[20] A. Collado and A. Georgiadis, "Improving wireless power transmission efficiency using chaotic waveforms," 2012 IEEE/MTT-S International Microwave Symposium Digest, Montreal, QC, Canada, 2012, pp. 1-3.
[21] F. Bolos, J. Blanco, A. Collado and A. Georgiadis, "RF Energy Harvesting From Multi-Tone and Digitally Modulated Signals," in IEEE Trans. Microw. Theory Techn., vol. 64, no. 6, pp. 1918-1927, June 2016.
[22] A. S. Boaventura and N. B. Carvalho, "Maximizing DC power in energy harvesting circuits using multisine excitation," 2011 IEEE MTT-S International Microwave Symposium, Baltimore, MD, 2011, pp. 1-4.
[23] I. Lee, Y. Lee, D. Sylvester and D. Blaauw, "Battery Voltage Supervisors for Miniature IoT Systems," in IEEE Journal of Solid-State Circuits, vol. 51, no. 11, pp. 2743-2756, Nov. 2016.
[24] J. A. Hagerty, F. B. Helmbrecht, W. H. McCalpin, R. Zane and Z. B. Popovic, "Recycling ambient microwave energy with broad-band rectenna arrays," in IEEE Trans. Microw. Theory Techn., vol. 52, no. 3, pp. 1014-1024, March 2004.
[25] C. R. Valenta and G. D. Durgin, "Rectenna performance under power-optimized waveform excitation," 2013 IEEE International Conference on RFID (RFID), Penang, 2013, pp. 237-244.
[26] A. Boaventura, A. Collado, N. B. Carvalho and A. Georgiadis, "Optimum behavior: Wireless power transmission system design through behavioral models and efficient synthesis techniques," in IEEE Microwave Magazine, vol. 14, no. 2, pp. 26-35, March-April 2013.
[27] M. Ali, G. Yang and R. Dougal, "A new circularly polarized rectenna for wireless power transmission and data communication," in IEEE Antennas and Wireless Propagation Letters, vol. 4, no. , pp. 205-208, 2005.
[28] C. H. K. Chin, Quan Xue and Chi Hou Chan, "Design of a 5.8-GHz rectenna incorporating a new patch antenna," in IEEE Antennas and Wireless Propagation Letters, vol. 4, no. , pp. 175-178, 2005.
[29] Yu-Jiun Ren and Kai Chang, "New 5.8-GHz circularly polarized retrodirective rectenna arrays for wireless power transmission," in IEEE Trans. Microw. Theory Techn., vol. 54, no. 7, pp. 2970-2976, July 2006.
[30] Ji-Yong Park, Sang-Min Han and T. Itoh, "A rectenna design with harmonic-rejecting circular-sector antenna," in IEEE Antennas and Wireless Propagation Letters, vol. 3, no. 1, pp. 52-54, Dec. 2004.
[31] J. O. McSpadden, Lu Fan and Kai Chang, "Design and experiments of a high-conversion-efficiency 5.8-GHz rectenna," in IEEE Trans. Microw. Theory Techn., vol. 46, no. 12, pp. 2053-2060, Dec 1998.
[32] Dawoud, Mahmoud M, "High frequency radiation and human exposure." In Proceedings of the International Conference on Non-Ionizing Radiation at UNITEN (ICNIR 2003), pp. 1-7. 2003.
[33] M. Fernandez, H.G. Espinosa, D.V. Thiel, and A. Arrinda, "Wearable slot antenna at 2.45 GHz for off-body radiation: Analysis of efficiency, frequency shift, and body absorption." Bioelectromagnetics 39, no. 1, pp. 25-34. 2008.
[34] K. Shiba, T. Nagato, T. Tsuji, and K. Koshiji, "Analysis of specific absorption rate and current density in an energy transmission system for a wireless capsule endoscope." In 2007 29th Annual International Conference of the IEEE Engineering in Medicine and Biology Society, pp. 6051-6054, 2007.
[35] IEEE Standards Coordinating Committee 34. "IEEE Recommended Practice for Determining the Peak Spatial-average Specific Absorption Rate (SAR) in the Human Head from Wireless Communications Devices: Measurement Techniques." Institute of Electrical and Electronic Engineers, 2003.
[36] B. Xu, Z. Kun, H. Sailing, and Y. Zhinong, "Understandings of maximum spatially-averaged power density in 5G RF EMF exposure study." In 2017 International Workshop on Antenna Technology: Small Antennas, Innovative Structures, and Applications (iWAT), pp. 115-117, 2017.

Samuel A. Rotenberg was born in Paris, France. He received an engineer diploma in Digital and Numeric Engineering System from the engineering school ENSEM in France, in 2016. He also received an M.Sc degrees in Mobile communication from Heriot-Watt University, Edinburgh, Scotland, in 2016. He received in 2017 the young scientist award at the international conference URSI GASS in Canada for his previous work. He is currently finalizing his PhD in telecommunication engineering and co-founder of INFINECT, a spinout company from Heriot-Watt University developing Flat Panel Antenna for Satellite Communication On the Move.

Symon K. Podilchak (S'03–M'05) received the B.A.Sc. in Engineering Science from the University of Toronto, ON, Canada, in 2005. While studying at Queen's University in Kingston, Ontario, Canada he received a M.A.Sc. and a Ph.D. in electrical engineering in 2008 and 2013, respectively, and he received the Outstanding Dissertation Award for his Ph.D. from the same institution. From 2013 to 2015 Symon was an Assistant Professor at Queen's. He then joined Heriot-Watt University, Edinburgh, Scotland, UK in 2015 as an Assistant Professor and became an Associate Professor in 2017. His research is also supported by a H2020 Marie Sklodowska-Curie European Research Fellowship, and, is currently a Senior Lecturer with The University of Edinburgh, School of Engineering.

He is a registered Professional Engineer (P.Eng.) and has had industrial experience as a computer programmer, and has designed 24 GHz and 77 GHz automotive radar systems with Samsung and Magna Electronics. Recent industry experience also includes the design of high frequency surface-wave radar systems, professional software design and implementation for measurements in anechoic chambers for the Canadian Department of National Defence and the SLOWPOKE Nuclear Reactor Facility. Dr. Podilchak has also designed new compact multiple-input multiple-output (MIMO) antennas for wideband military communications, highly compact circularly polarized antennas for microsatellites with COM DEV International, as well as new wireless power transmission systems for Samsung. His research interests include surface waves, leaky-wave antennas, metasurfaces, UWB antennas, phased arrays, and CMOS integrated circuits.

Dr. Podilchak and his students have been the recipient of many best paper awards and scholarships; most notably Research Fellowships from the IEEE Antennas and Propagation Society, the IEEE Microwave Theory and Techniques Society as well as the European Microwave Association. Dr. Podilchak also received a Postgraduate Fellowship from the Natural Sciences

and Engineering Research Council of Canada (NSERC) and five Young Scientist Awards from the International Union of Radio Science (URSI). In 2011 and 2013 he received student paper awards at the IEEE International Symposium on Antennas and Propagation, and in 2012, the Best Paper Prize for Antenna Design at the European Conference on Antennas and Propagation for his work on CubeSat antennas, and in 2016, received The European Microwave Prize for his research on surface waves and leaky-wave antennas. In 2017 and 2019 Dr. Podilchak was bestowed a Visiting Professorship Award at Sapienza University in Rome. In 2014, the IEEE Antennas and Propagation Society recognized Dr. Podilchak as an Outstanding Reviewer for the IEEE Transactions on Antennas and Propagation. Dr. Podilchak was also the founder and First Chairman of the IEEE Antennas and Propagation Society and the IEEE Microwave Theory and Techniques Society, Joint Chapter of the IEEE Kingston Section in Canada as well as Scotland. In recognition of these services, the IEEE presented Dr. Podilchak with an Outstanding Volunteer Award in May 2015. Currently he also serves as a Lecturer for The European School of Antennas and is an Associate Editor to the journal IET Electronic Letters.

Pascual D. Hilario Re was born in Murcia, Spain. He received the B.Eng. and the M.Sc. degrees in telecommunications engineering from the Universidad Politcnica de Cartagena, Spain, in 2012 and 2015, respectively. He also received the Ph.D. degree from Heriot-Watt University, Edinburgh, Scotland, UK, in 2019. His current research interests include retrodirective systems, wireless power transmission applications, automotive radar, and analysis and design of power amplifiers.

George Goussetis (S'99–M'02–SM'12) received the Diploma degree in electrical and computer engineering from the National Technical University of Athens, Greece, in 1998, the B.Sc. degree in physics (Hons.) from University College London, U.K., in 2002, and the Ph.D. degree from the University of Westminster, London, U.K., in 2002. In 1998, he joined Space Engineering, Rome, Italy, as an RF Engineer, and as a Research Assistant with the Wireless Communications Research Group, University of Westminster, U.K., in 1999. From 2002 to 2006, he was a Senior Research Fellow with Loughborough University, U.K. He was a Lecturer (Assistant Professor) with Heriot-Watt University, Edinburgh, U.K., from 2006 to 2009, and a Reader (Associate Professor) with Queen's University Belfast, U.K., from 2009 to 2013. In 2013, he joined Heriot-Watt, as a Reader, and was promoted to Professor, in 2014.

He has authored or co-authored over 200 peer-reviewed papers five book chapters one book and two patents. His research interests include the modeling and design of microwave filters, frequency-selective surfaces and periodic structures, leaky wave antennas, microwave sensing and curing as well numerical techniques for electromagnetics. Dr. Goussetis has held a research fellowship with the Onassis Foundation in 2001, a research fellowship with the U.K. Royal Academy of Engineering from 2006 to 2011, and a European Marie-Curie experienced researcher fellowship from 2011 to 2012. He was a co-recipient of the 2011 European Space Agency Young Engineer of the Year Prize, the 2011 EuCAP Best Student Paper Prize, the 2012 EuCAP Best Antenna Theory Paper Prize, and the 2016 Bell Labs Prize.

Jaesup Lee received the M.S. degree in electrical engineering from the University of California at Los Angeles, Los Angeles, CA, USA.,He is currently with the Samsung Advanced Institute of Technology, Suwon, South Korea. His current interests include RF and analog circuits, especially ultralow-power personal network platforms and RF wireless power transfer.